Proceedings from the University of Washington
School of Oceanography Senior Thesis, Academic Year 2011-2012

Coastal Upwelling of Magdalena Bay, Mexico, in a La Niña year

William Jay Kammin

[1]*University of Washington, School of Oceanography,*
Box 355351, Seattle, Washington 98195
[*]Will.kammin@gmail.com

Received June 2012

NONTECHNICAL SUMMARY

Coastal Upwelling is an oceanographic phenomenon caused by alongshore wind stress and the Coriolis effect. This results in the divergence of surface water away from the coast. The divergence of surface water must be balanced by the inflow of deeper, usually nutrient rich, water which flows upward into the surface layer of the ocean. Coastal upwelling is known to cause phytoplankton blooms which support large coastal fisheries around the west coast of the world's continents. For this reason upwelling is used by fisheries managers to predict primary productivity in many ecosystems.

Upwelling off Magdalena Bay on the west coast of Baja Mexico was investigated and the magnitude of upwelling calculated. From March 20-21st the R/V Thomas G. Thompson cruised from the coast north of Magdalena Bay toward the southern tip of Baja. Two transects bounded the coast in order to calculate the volume of water transported off shore (Figure 1). The Magdalena Bay area was chosen due to consistent upwelling in the area caused by favorable shore orientation, winds, and bathymetry (Figure 4). Water velocity was recorded using the ship's Acoustic Doppler Current Profiler (ADCP). Satellite and Conductivity-Temperature-Depth (CTD) data was used to find the common signatures of upwelling; lower sea surface temperature and shallower thermocline structure. Anomalously cool water along the equator, caused by La Nina, can reinforce winds and increase upwelling in the area.

Estimates by the Pacific Environmental Fisheries Laboratory's Coastal Upwelling Indices showed expected upwelling magnitudes of 144,123 m^3/s. Ekman transport of 238,286 m^3/s was found in the study area. Understanding how the strength of global climate phenomenon correlate to local upwelling conditions can help fisheries and environmental managers more accurately predict potential production in coastal ecosystems.

ABSTRACT

Upwelling near Magdalena Bay, Mexico was calculated from March 20-21st. The hydrography of the area was investigated using Conductivity-Temperature-Depth (CTD) casts from the R/V Thomas G. Thompson. An Acoustic Doppler Current Profiler (ADCP) was used to detect current velocity and estimate the magnitude of upwelling. Southern and eastern transects were made starting at the northern tip of the Cape of Magdalena. Sea surface temperature collected with the CTD was used along with AVHRR satellite imagery to identify areas of upwelling by way of 17.5°C isotherms. A storm from March 16-17 increased wind stress in the region and likely upwelling. Coastal station sea surface temperatures were 1.8-2.7°C cooler than offshore waters indicating upwelling. Total volume of upwelled water was found using mass balance equations and the ADCP measured currents. Upwelling of 0.184 Sverdrup's (Sv) was

found during the cruise which is higher than the Pacific Fisheries Environmental Laboratories estimate of ~0.144 Sv of upwelling. Higher than predicted coastal upwelling may have been caused by a tongue of cold water in the study area. This cold tongue may have increased the water transport out of the study area. Upwelling is responsible for high productivity along the California Current System (CCS). It is believed that increased upwelling can enhance productivity and produce a net sink of CO_2 in upwelling regions. Continued study of upwelling in this area will help us better understand the regional impact of global scale ENSO phenomenon as scientists look to mitigate the impacts climate change.

Figure1. Stations of senior research cruise used bounding the study area. CTD casts were taken at each station.

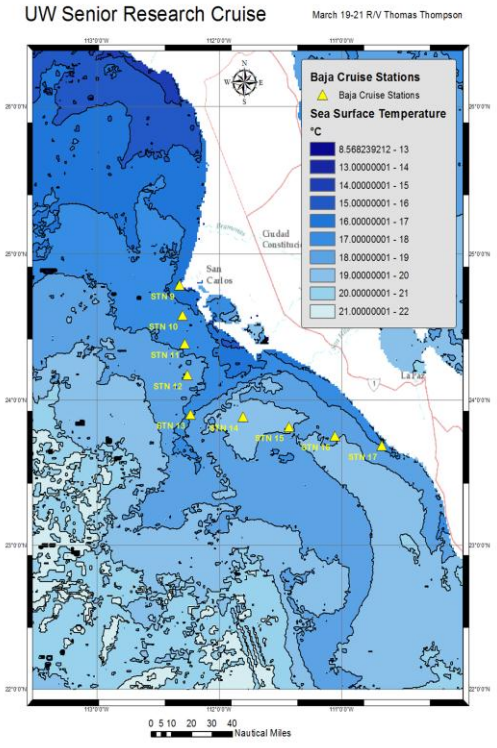

Coastal Upwelling is an oceanographic phenomenon caused by alongshore wind stress and the Coriolis effect, which results in the divergence of surface water away from the coast (Figure 4). Upwelling can enhance local productivity by replenishing nutrients, which can lead to much longer periods of sustained growth than would otherwise be possible (Mote and Mantua, 2002). The Baja peninsula is at the terminal end of the California Current System (CCS) and experiences upwelling typical of an eastern boundary current ecosystem. The area has relatively low wind stress and surface currents, (Kessler, 2002; Kessler, 2006). However, the regional upwelling is still strong enough to support rich coastal fisheries. Coastal upwelling has a very strong impact on the physical and ecological structure in the eastern boundary current ecosystem (Schwing and Mendelssohn, 1997). During spring and summer upwelling the local circulation, thermohaline structure, and mass balance are driven by upwelling favorable winds. This area has shown a strong correlation between upwelling and the El Niño Southern Oscillation (ENSO) cycle, with increased upwelling during the La Niña phase (Schwing et al., 2000). Variability on an inter-annual timescale is largely attributed to the ENSO cycle and long term climate change (Mantua and Hare 2002; (Schwing and Mendelssohn, 1997; Godinez et al. 2010).

Ocean upwelling off the coast of Baja California was calculated from March 19-21 to compare to the Pacific Fisheries Environmental Laboratory's (PFEL) regional coastal upwelling indices (CUI) and models. The CUI is derived from wind stress fields (ASCAT satellite) and modeled by PFEL to create coastal upwelling magnitudes for fisheries management organizations. Most permanent upwelling zones along the Baja Peninsula are located down current of capes on the western coast (Zaytsev et al. 2003). The Magdalena Bay transects of Baja Mexico were analyzed due to an upwelling favorable shoreline angle and favorable monthly average wind stress (Figure 4). Local winds along the Baja Peninsula are equator ward on average and reach a maximum in late spring (King et al. 2011). Temperature, salinity, and density profiles were collected along the coast and on 2 transects near Magdalena Bay (Figure 1). Conductivity- temperature-pressure (CTD) data, wind speed, and Acoustic Doppler Current Profiler (ADCP) data were collected during the entirety of the cruise. Isopycnals (lines of constant density) and ADCP data were used to find upwelling in these areas (Figure 5, 6). CTD data was used to

Figure 2: Panels show the progression of Sea Surface Temperature from March 19-22 with 1km resolution provided by NASA Jet Propulsion Laboratory. (*sst.jpl.nasa.gov*)

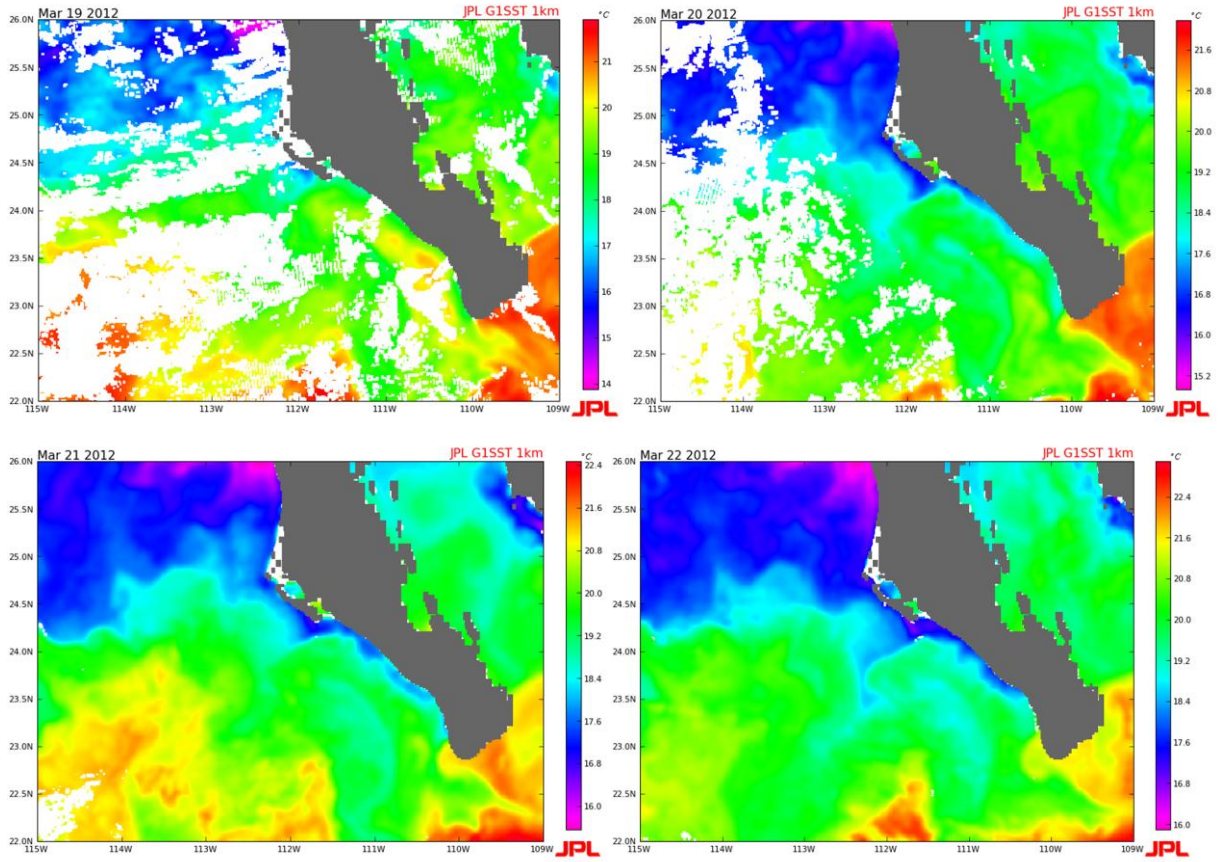

find the common signatures of upwelling; lower sea surface temperature and shallower thermocline structure. The data was used to synthesize a picture of surface currents and the magnitude of upwelling along the coast of Baja California. There is currently debate in the oceanographic community as to whether the ENSO cycle will increase or decrease coastal upwelling in the CCS. Mote and Mantua (2002) have argued that drastic changes in upwelling are unlikely in the CCS while Bakun (1990) has suggested that upwelling is likely to strengthen significantly. Due to current La Nina conditions upwelling magnitude was analyzed to confirm whether or not upwelling would be significantly higher or lower compared to previous studies in the Baja region. Calculated upwelling magnitude can be used to compare to the CUI which is a rough proxy for productivity along the continental shelf of Baja. Examining the upwelling in this area will give us a better understanding between local upwelling and La Niña conditions.

METHODS

CTD Data

To bound the coast 2 transects consisting of 9 stations were completed (Figure 1). Mounted to the ship's rosette was a Sea-Bird Electronics 911*plus* CTD sensor package. The CTD rosette was deployed at each station down to at least 400m depth unless constrained by the sea floor. Temperature, salinity, oxygen and density data were collected. The data were used to describe the structure of the pycnocline, thermocline and halocline in the water column along the path of the

2 transects from coastal to ocean waters. The stratification data was then used to find isotherms or isopycnals to define the bottom of the Ekman layer along the ships track. A temperature change of >0.1°C/m depth was used to define the top of the thermocline and the bottom of the Ekman layer. The bottom of the thermocline was defined as a <0.1°C/m depth change, indicating the end of rapid temperature changes. Using isotherm boundaries, the flow above and below the thermocline was analyzed with the ADCP.

Figure 3: Diagram of upwelling processes in the study area. The thermocline (red line) is shown being above and below the level shallowest measurement (grey line).

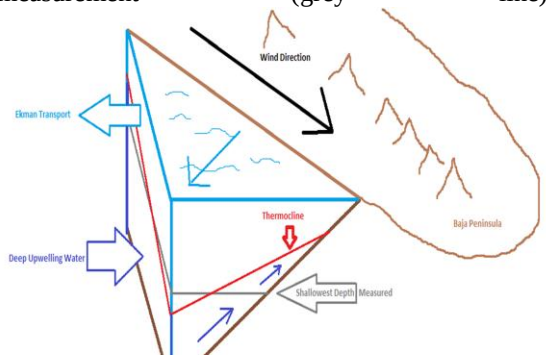

ADCP Data

A ship mounted RDI Ocean Surveyor 75KHz ADCP was used to collect velocity profiles on the cruise. The ADCP can accurately measure flow (±1.0%, ±0.5cm/s) in and out of the study area which allowed calculation of upwelling through mass balance equations. The ADCP ran continuously throughout the cruise. Using the coast and the transect lines as boundaries; an imaginary triangle around the cape of Magdalena was created. The calculation of the flow perpendicular to our track allowed us to analyze volume into and out of the study triangle. Using the definition of the thermocline described above, the thermoclines top and bottom was averaged between stations. By averaging the depth of the top and bottom of the thermocline a variable thermocline depth between stations was created for the study. The magnitude of currents perpendicular to the ships track were then calculated between stations. By multiplying the variable thermocline depth between stations by the observed average ADCP current between stations, the total flux of water into and out of the study area was found.

Satellite Data

Sea Surface Temperature (SST) from Moderate Resolution Imaging Spectroradiometer (MODIS) Aqua satellite and Advanced Very High Resolution Radiometer (AVHRR) satellites were used to find areas of likely upwelling by identifying colder coastal waters close to shore (Figure 1,2). AVHRR infrared images have a nadir resolution of 1.1 km. The NOAA Coastwatch program (coastwatch.pfeg.noaa.gov) provided the processed satellite data products used during ship operations and afterward for data processing. The MODIS satellite also provided chlorophyll concentrations for the study.

Figure 4: NOAA/NDCC 3 day composite wind stress centered on 3-20-2012 00:00:00. Consistent winds were running parallel to shore in the study area driving coastal upwelling. (*coastwatch.pfeg.noaa.gov*)

RESULTS

Hydrography

Prevailing winds averaged ~8 m/s and 145° from north over the course of the study (Figure 4). Offshore stations 11-15 had surface temperatures ranging from 17.9°C to 19°C (Figure 2, Figure 5 a). Station 13 exhibited strong southwesterly current in the surface layer and had a low surface temperature of 17.9°C. Coastal station 9 was 1°C cooler than station 10. Coastal station 17 had a surface temperature of 17.2°C and was 1.1°C cooler than station 16. The cooling trend was verified through JPL 1km SST products (Figure 2).The bottom of the mixed layer ranged from 52m to 14m with shallower mixed layers near shore. The bottom of the mixed layer also represents the depth range of the top of the thermocline (Figure 5 b). The average for the top of the thermocline was 31m. The bottom of the thermocline ranged from 52-90m depth with an average of 71m depth. The 25 sigma-theta value ranged from a depth of 60m to 0m with the shallow isopycnal surfaces appearing near shore (Figure 5 b). Nitrate values between 50-100m depth ranged between 2-28.4 umol/L with surface values of 0-1.71 umol/L. The highest surface Nitrate values were found at coastal station 9 and station 16.

Figure 5: a) Station Temperature Profiles from CTD casts. b)Section profiles of transect density contours (stations 9-17). c) Map of station locations. d) Section profile of temperature.

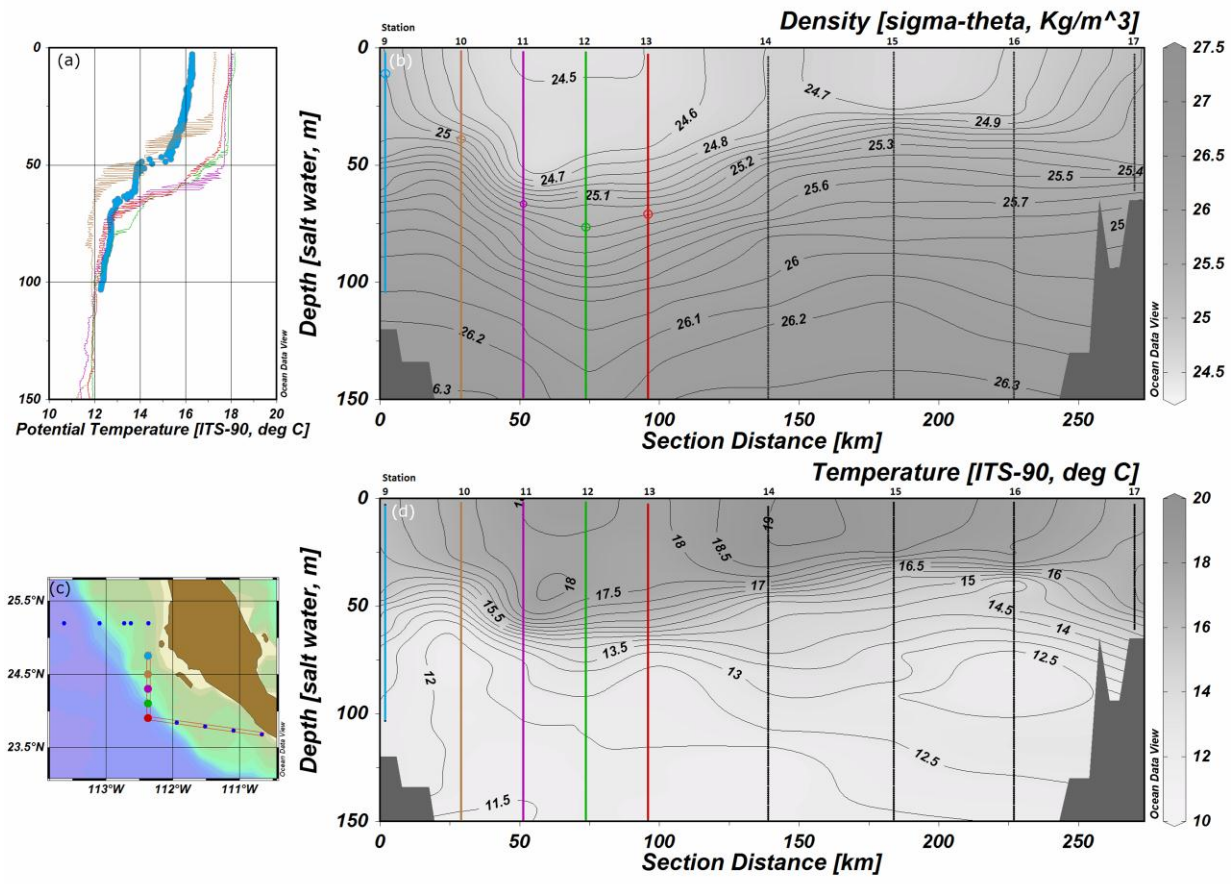

Currents

ADCP data revealed variable currents throughout the transect (Figure 6). Total average currents from 35-350m were .016 m/s west and .005 m/s north. Average currents from 35-85m between stations 9 and 13 were east .053 m/s and south .005m/s. Average currents from 35-85m between stations 13 and 17 were west .067 m/s and south .032 m/s (Figure 6). The main component of currents along northern transect (stations 9-13) was easterly. Strong southwest currents were found down to 100m along the southern transect (stations 13-17). Volume calculated entering the study area from 35m-67m was 0.184 Sv. Using the variable thermocline depth a volume transport of 0.238 Sv was measured. PFEL coastal upwelling index (CUI) was averaged over the time period of the study and produced an average value of 68.6 $m^3/s/100m$ of coastline which corresponds to a volume transport of 0.144 Sv. With values of .184 Sv ±.027 Sv and .238 Sv ±.027 Sv we expect CUI values of 87-113 $m^3/s/100m$ of coastline with an error of ±13 $m^3/s/100m$.

Figure 6: ADCP current data in m/s averaged from 35-60m (Cyan) and 60-84m (Blue) along the ships track.

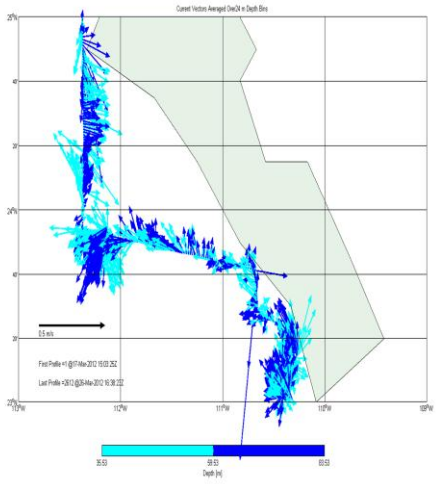

Satellite

Satellite images show 17.5°C water along the shoreline of the study area indicating upwelling over the entire coastal region (Figure 2). A large tongue of cold water protruded from the coast to station 13. High chlorophyll concentrations are also seen in all of the cold coastal waters as well as the cool water tongue (Figure 7).

DISCUSSION

A storm occurred during March 16-17th along the Baja Coast. This storm created strong upwelling signatures that were present at stations 9, 13 and 17 with surface temperatures of 16.3°C, 17.9°C and 17.26°C respectively. Each station had a SST >1°C cooler than the next closest station. Coastal stations sea surface temperatures (SST) were 1.8-2.7°C cooler than offshore waters, indicating upwelling. Decreasing mixed layer depth was also present in the coastal station. Throughout the study region satellite temperatures along the coast were 17.5°C and cooler (Figure 1, 2) implying upwelling along the entire coastline of the survey. Station 13 experienced strong surface currents and a deep thermocline at 60m depth. 60m depth corresponds to the sigma-theta value of 25 kg/m^3.The 25 kg/m^3 sigma isopycnal runs all the way to the surface at stations 9 and 17 (Figure 5 b). This provides a path of least resistance for >60m depth water to travel eastward and upwell into the mixed layer. The increased surface nutrients at coastal stations 9 and 16 and 17 show how upwelling can provide nutrients to primary producers in an upwelling ecosystem.

The lowest depth of measured currents from the ship's ADCP is 35-43m depth. This effectively limits the study of currents to below the Ekman layer for the majority of stations. The other main limiting factor was the inability to account for tidal currents due to the short time period of the survey. Unfortunately, this makes it difficult to accurately measure the magnitude of surface flow. Because

of this constraint, we have had to rely on the assumption that inflow must be equal to outflow in the study area. The calculated values of 0.184 Sv upwelling from 35-67m and 0.238 Sv with a variable depth thermocline suggest that upwelling was stronger than predicted by the PFEL's CUI. The large range in transport values suggest the method of quantifying the size of the inflow layer is very important. The most likely explanation for increased upwelling in the area is the cold tongue observed in satellite images during the course of the study (Figure 1, 2).

Station 13 may reside in, or be in close proximity to, a jet of upwelled water. Satellite images show a tongue of cold water present throughout the survey (Figure 2). Upwelling jets have been known to transport many times the volume of water expected compared to wind stress dynamics alone (Barth, J. A. and S. D. Pierce. 2000). The jet is likely a momentum based remnant of the storm that preceded the study. CUI values between the 14^{th} and 17^{th} of March had Ekman transport values as high as 250 m^3/s/100m of coastline in the 6 hour products provided by the PFEL (*http://las.pfeg.noaa.gov*)and 160 m^3/s/100m of coastline for daily products (Figure 4). The cold tongue's southwesterly orientation, 45° to the right of wind stress suggests that surface Ekman transport is driving the cold tongue feature. Chlorophyll maximums could also be identified in satellite images and were highest in the areas of coastal upwelling and the cold tongue (Figure7). Between stations 13 and 14 current speeds reached a maximum of .09 m/s out of the study area. This was the highest average current speed found transporting water out of the study area. The total volume of water transported out of the area between stations 13 and 14 was 0.182 Sv between 35 and 75m depth. The measurements between these stations are likely skewed due to tides. When the CTD profile was being cast at station 13 ebb tide was halfway complete. This suggests offshore tidal currents were near their peak. Features like this cold tongue reinforce the need to continue in-situ measurements rather than relying on atmospheric forcing models like the PFEL's CUI. Though global climate models are helpful for understanding large scale processes spatial resolution of 100km is common. With such a large resolution regional, observation based, modeling projects are necessary to gain insight into coastal ecosystems. Without in-situ measurements features like jets, upwelling eddies and tidal mixing cannot be fully captured which limits the accuracy of modeled estimates (King et al, 2011).

Primary productivity due to upwelling has been suggested as a sink for CO_2 but it has been found in the central CCS that the source vs. sink nature of the CCS corresponds with ENSO conditions (Ribas-Ribas et al, 2011). The CCS becomes a source of CO_2 in El Nino years and a sink of carbon in La Nina years. If upwelling drives higher productivity then the flux of carbon sequestered into seafloor sediment may be a negative feedback to anthropogenic CO_2 production.

Though the area of upwelling is clearly defined in satellite images, a lack of stations further off shore creates low spatial resolution for describing salinity and temperature based geostrophic flow. Also, a lack of corroborating nutrient data across the survey limits the ability to calculate nutrient flux. It will be difficult to accurately estimate the total flux of nutrients caused by upwelling without measuring surface currents and increasing nutrient samples. Without these key parameters analyzing the effect of upwelling on carbon sequestering and primary productivity are difficult to ascertain and remain beyond the scope of this study.

Without the time constraints of the cruise more stations and a larger sampling area could have increased the accuracy of measured upwelling. Significant components of variation are due to inter-annual variability such as the ENSO cycle (Godinez et al. 2010). Greater spatial and temporal scales would provide more information about the

impacts of the ENSO cycle in the Eastern Tropical North Pacific. The fact that it is almost impossible to correlate one storm system over 3 days to a global phenomenon limits the ability to enhance our understanding of regional climatic dynamics.

CONCLUSIONS

Clear skies above Baja California made the extent of upwelling along the coast clear in satellite images. Water 17.5°C and cooler was present along the entire coastline of the study area indicating strong upwelling. The study revealed:

- Calculated upwelling of 0.238 Sv was higher than the PFEL CUI of 0.144 Sv.
- Coastal station SSTs were 1.8-2.7°C cooler than offshore waters.
- Nutrient concentrations in upwelling stations were higher than surrounding stations.
- A large cold tongue driven by wind stress may have caused the higher than expected upwelling.
- Chlorophyll maximums were found in upwelling waters.
- Tides were not accounted for in this study and bring considerable uncertainty to the current magnitudes reported.

The chlorophyll maximums evident in the colder upwelling water showed the increased productivity associated with upwelling. Magdalena Bay shows the classic dynamics that make upwelling coastlines so productive. Nutrient flux into shallow water fuels this coastal ecosystem. Creating a larger study area with more interdisciplinary measurements at each station will further enhance our understanding of the ecosystem. More observational in-situ measurements and interdisciplinary collaboration between scientists, sea gliders, satellites, ships and moorings can help refine our understanding of complicated processes such as jets, tidal mixing, and primary productivity in the coastal environment. Incorporating these suggestions should allow future studies to develop a greater understanding of the physical, chemical and biological components of oceanography in the area.

ACKNOWLEDGEMENTS

I would like to thank all my professors especially Charlie, Julie, and Rick. Many thanks go out to the Captain and crew of Tommy G. Thompson. I would also like thank Sara G, Logan S, Matt R, and Eric Engel as well as the rest of my Ocean 444 classmates.

Figure 7: Panels show the progression of Sea Surface Temperature from March 19-22 with 1km resolution provided by NASA Jet Propulsion Laboratory. (*sst.jpl.nasa.gov*)

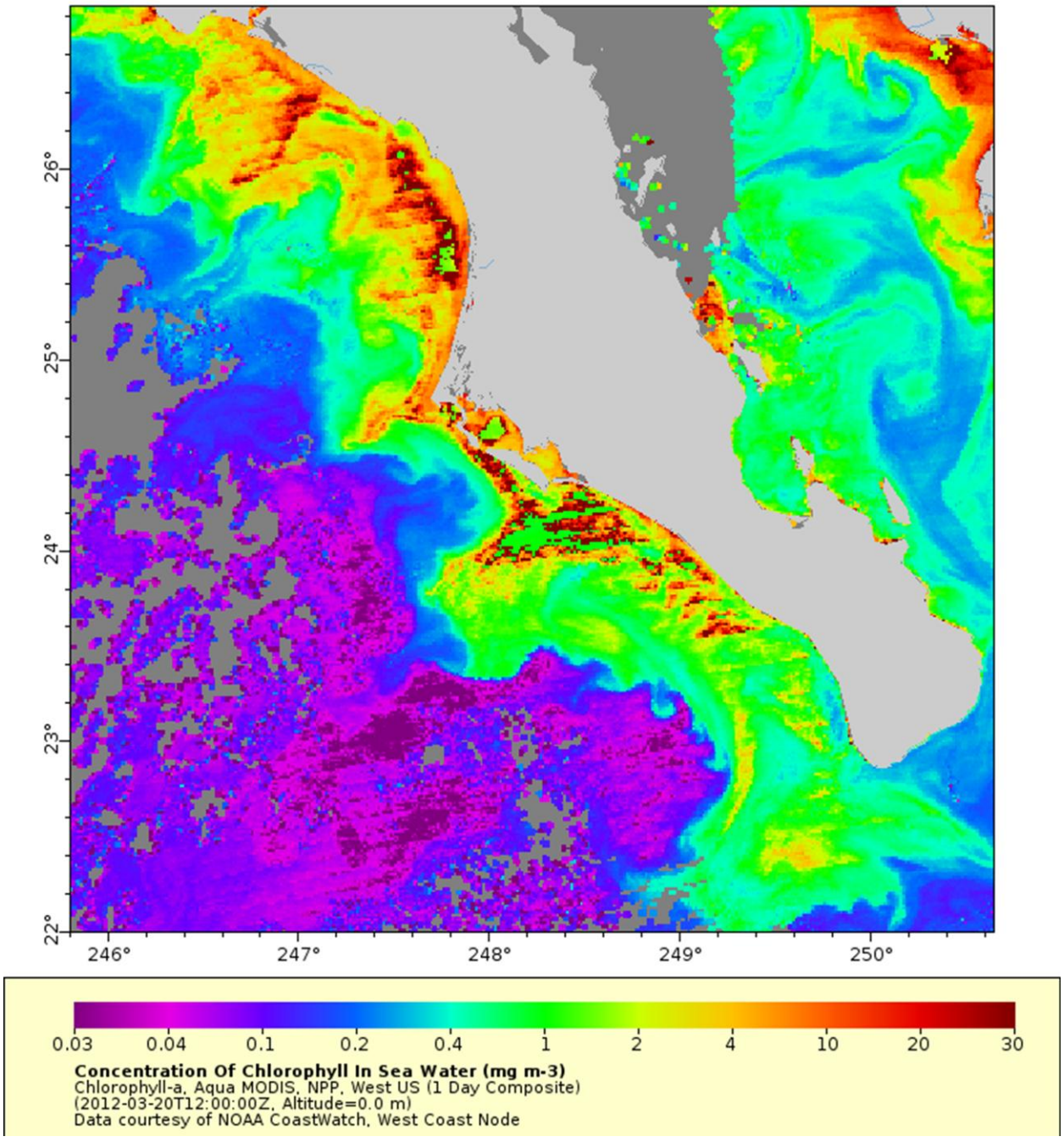

REFERENCE LIST

Bakun, A. 1990. Global climate change and intensification of coastal ocean upwelling. Science. **247:** .

Barth, J. A. and S. D. Pierce. 2000. A separating coastal upwelling jet at Cape Blanco, Oregon and its connection to the California Current System. **47:** .

Godinez V.M., Lavin M.F., Kurczyn J.A. and Beier E. 2010. Circulation at the entrance of the Gulf of California from satellite altimeter and hydrographic observations. **115:** .

Kessler, W. S. 2002. Mean Three-Dimensional Circulation in the Northeast Tropical Pacific. J. Phys. Oceanogr. **32:** 2457-2471.

Kessler, W. S. 2006. The circulation of the eastern tropical Pacific: A review. **69:** 181.

King, J. R., V. N. Agostini, C. J. Harvey, G. A. McFarlane, M. G. G. Foreman, J. E. Overland, E. Di Lorenzo, N. A. Bond and K. Y. Aydin. 2011. Climate forcing and the California Current ecosystem. ICES J. Mar. Sci. **68:** 1199-1216.

Mantua, N. J. and S. R. Hare. 2002. The Pacific decadal oscillation. J. Oceanogr. **58:** 35-44, doi:10.1023/A:1015820616384.

Mote, P. W. and N. J. Mantua. 2002. Coastal upwelling in a warmer future (DOI 10.1029/2002GL016086). Geophys. Res. Lett. **29:** 53.

Ribas-Ribas, M., J. M. Hernandez-Ayon, V. F. Camacho-Ibar, A. Cabello-Pasini, A. Mejia-Trejo, R. Durazo, S. Galindo-Bect, A. J. Souza, J. M. Forja and A. Siqueiros-Valencia. 2011. Effects of upwelling, tides and biological processes on the inorganic carbon system of a coastal lagoon in Baja California. Estuar. Coast. Shelf Sci. **95:** 367-376.

Schwing, F. B. and R. Mendelssohn. 1997. Increased coastal upwelling in the California Current System. **102:** 3421-3438, doi:10.1029/96JC03591.

Schwing, F., C. Moore, S. Ralston and K. Sakuma. 2000. Record coastal upwelling in the California Current in 1999. **41:** 148-160.

Zaytsev, O., R. Cervantes-Duarte, O. Montante and A. Gallegos-Garcia. 2003. Coastal Upwelling Activity on the Pacific Shelf of the Baja California Peninsula. J. Oceanogr. **59:** 489-502.